Materials Transactions, JIM, Vol. 38, No. 10 (1997), pp. 879 to 885

Refinement and Localization of Primary Intermetallic Compound in Hyperperitectic Al-Cr Alloy by Centrifugal Duplex Casting†

Tatsuya Ohmi, Yoshiaki Kimura††, Youichi Itoh, Masayuki Kudoh and Kiyotaka Matsuura

Division of Materials Science and Engineering, Graduate School of Engineering, Hokkaido University, Sapporo 060, Japan

A novel process named Centrifugal Duplex Casting has been proposed: It is a manufacturing process of an aluminum cast pipe with an *in-situ* composite layer which contains fine intermetallic crystals. In this process, two kinds of molten metal, i.e. molten aluminum (the first melt) and molten Al-Cr alloy with higher liquidus temperature (the second melt), are cast in sequence at a given interval into the rotating mold of a centrifugal caster. The second melt collides with the meniscus of the first melt, and is dispersed as a great number of fine fluid clumps. These fluid clumps are rapidly quenched, migrate toward the outer periphery, and accumulate to form the composite layer. The particle size of the intermetallic crystals in this composite layer is much smaller than that of the Al-Cr alloy centrifugally cast by a conventional process. The solidification structure of the cast pipe produced by Centrifugal Duplex Casting is controlled by cooling capacity of the first melt. For instance, when the first melt has superheat at the moment of the second-melt casting, coarse intermetallic crystals grow inside of the refined composite layer. On the other hand, when the first melt has partially been solidified, the growth of the intermetallic crystals is suppressed. Therefore, the time interval between the two casting operations is an important parameter in this process.

(Received May 2, 1997)

Keywords: *composite material, intermetallic compound, hyperperitectic aluminum-chromium alloy, centrifugal casting, mixing, rapid solidification, refinement, structure control, solidification*

I. Introduction

During the solidification of hypereutectic or hyperperitectic aluminum-transition metal alloys, hard particles of primary intermetallic compounds are crystallized. Recently, researchers have investigated the use of centrifugal casting of these alloys to produce tubular *in-situ* composite castings in which the primary intermetallic crystals are concentrated near the outside surface[1)-3)]. These "surface composite castings" [4] are expected to be heat-resistant or wear-resistant aluminum-base materials. However, localization of the primary crystals is incompatible with rapid solidification in the conventional centrifugal casting process because migration of the primary crystals takes time. Therefore, the primary crystals tend to grow to a considerable size, deteriorating the strength and machinability of the castings.

In this study, we developed a new process to concentrate the fine intermetallic crystals near the outer periphery of the cast pipes. We named this process "Centrifugal Duplex Casting" (CDC process). This process is a hybrid of the centrifugal casting and Duplex Casting. The latter is effective for the refinement of primary crystals in cast alloys, as we have already reported[5].

II. Principles of the CDC Process

An Al-Cr alloy was used in this study. Figure 1 shows an aluminum-side portion of an Al-Cr phase diagram[6]. In the aluminum-rich Al-Cr alloy, the final solidification reaction is a peritectic reaction (liquid phase + Al_7Cr → Aluminum solid solution). Therefore, analysis of the structure formation of this alloy is easier than that of a hypereutectic alloy such as an Al-Fe or Al-Ni alloy in which intermetallic compounds are also crystallized in

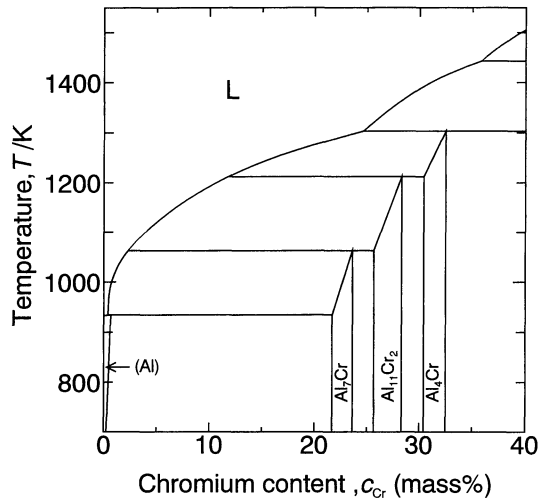

Fig. 1 Aluminum-side portion of the Al-Cr phase diagram[6].

† This paper was originally published in Japanese in J. Japan Inst. Metals, **60** (1996), 490.

†† Graduate Student, Hokkaido University. Present address: Nippon Steel Co., Ltd., Kimitsu 299-11, Japan.

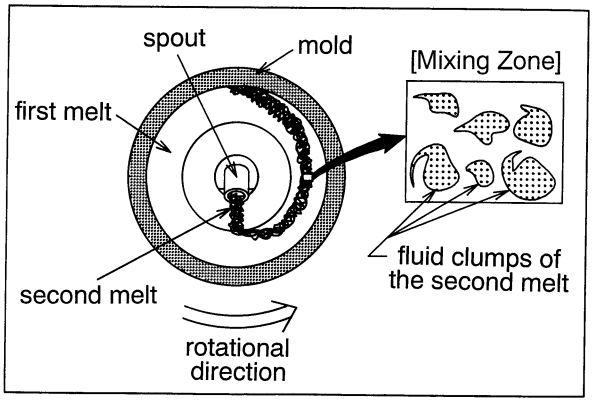

Fig. 2 Schematic illustration of the basic concept of the CDC process.

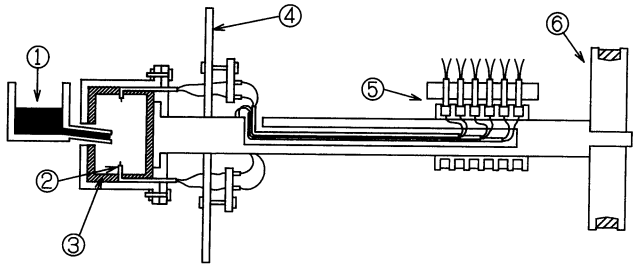

Fig. 3 Schema of the mold and main shaft of the centrifugal caster. ① melt, ② thermocouple, ③ mold (insulation brick), ④ heat-shielding plate, ⑤ slip ring, ⑥ pulley.

the eutectic reaction.

In the CDC process, two kinds of molten metals with different compositions are cast in sequence at a given interval into the rotating mold of a centrifugal caster. For this study, molten aluminum was used for "the first melt", which was cast first, and a hyperperitectic Al–Cr alloy melt with a high liquidus temperature was used for "the second melt", which was cast later. Figure 2 shows the basic concept of this process, illustrating the way in which the second melt mixes with the first melt already cooling in the mold. The second melt collides with the meniscus of the first melt, which is spinning at a high speed, and is dispersed as a great number of fine fluid clumps. These fluid clumps are rapidly quenched, migrate toward the outer periphery due to centrifugal force, and accumulate to form the composite layer with fine primary crystals. Through this mechanism, at the same time this composite layer is formed, the intermetallic crystals are also refined and localized.

In the Duplex Casting process, the first melt is partially solidified before the second melt is mixed. The solid phase in the first melt is remelted and absorbs the latent heat of fusion when it comes into contact with the second melt. The cooling of the second melt is promoted by this phenomenon[7]. In this research, we also focused our attention on this effect in the CDC process. We attempted to control the structure of the composite layer by changing the fraction solid of the first melt through an adjustment of the time interval between the two casting operations.

III. Experimental Method

Figure 3 shows a schematic view of the horizontal centrifugal caster used in the experiments. A cylindrical container made of insulation brick (80 mm in the inside diameter, taking the interior length 40 mm, and radial thickness 10 mm) was used for a mold. Thermocouples were located at 0, 5, and 10 mm from the inner wall in the radius direction of the mold, and the temperature of the specimen was measured through the slip ring mechanism. The mold was not preheated.

The rotation velocity of the mold was 19 s^{-1}, which arose gravity multiple of 59G as the centrifugal force at the outer periphery of the specimen.

We used pure Aluminum as the first melt and Al–10 mass%Cr or Al–20 mass%Cr alloy as the second melt. The mass ratio of the first melt to the second melt, W_1/W_2, was 3 or 7. The superheat of the first melt was 100 K above the liquidus, and that of the second melt was 50 K. The total mass of the poured melt was 336 g, and the radial thickness of the cast pipe was about 16 mm.

Centrifugally cast pipes of Al–2.5 mass%Cr alloy and Al–5 mass%Cr alloy, produced by means of the conventional process, were used as comparison specimens. The superheat of each alloy was set at 70 K.

The etchant, mixed in a ratio of H_2O:HCl:HNO_3:HF =50:15:25:10, was used to reveal the macrostructure of the specimens.

IV. Results and Discussion

1. The solidification structures of Al–Cr alloys centrifugally cast by the conventional process

Figures 4(a) and (b) show the macrostructures of the Al–2.5 mass%Cr alloy and the Al–5 mass%Cr alloy, respectively, which were produced by the conventional centrifugal casting process. The figures show the structures near the outer periphery on the transverse cross section of the specimens. In each specimen, the intermetallic crystals (black particles) concentrate on the outer side, and there are giant intermetallic crystals which are of the order of millimeters. The thickness of the layer where the intermetallic crystals are distributed is about 2 mm in the Al–2.5 mass%Cr alloy and about 5 mm in the Al–5 mass%Cr alloy. That is, the layer becomes thicker as the Cr concentration of the alloy increases.

Figures 5(a) and (b) show the microstructures of the composite layers of the Al–2.5 mass%Cr alloy and the Al–5 mass%Cr alloy, respectively. They show the back-scattered electron images obtained by using SEM. The compositional EPMA analysis revealed that the intermetallic compound in the Al–2.5 mass%Cr alloy is Al_7Cr phase. On the other hand, the intermetallic crystals which consist of $Al_{11}Cr_2$ and Al_7Cr are observed in the Al–5 mass%Cr alloy as shown in Fig. 5(b). These results do not agree with a report of Murata *et al.*[2] which claims

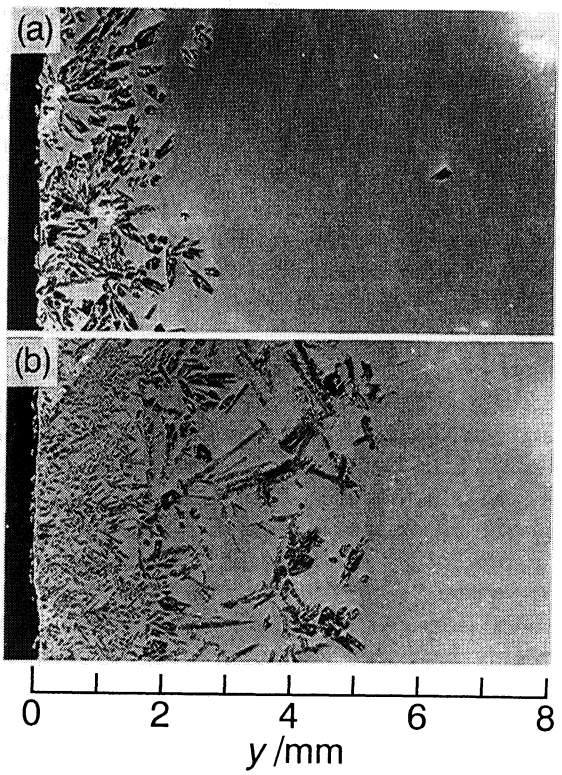

Fig. 4 Macrostructures showing the formation of intermetallic crystals near the outer periphery of the cast pipes produced by the conventional centrifugal casting. y: distance from the outer periphery of the cast pipe. (a) Al-2.5 mass%Cr alloy, (b) Al-5 mass%Cr alloy.

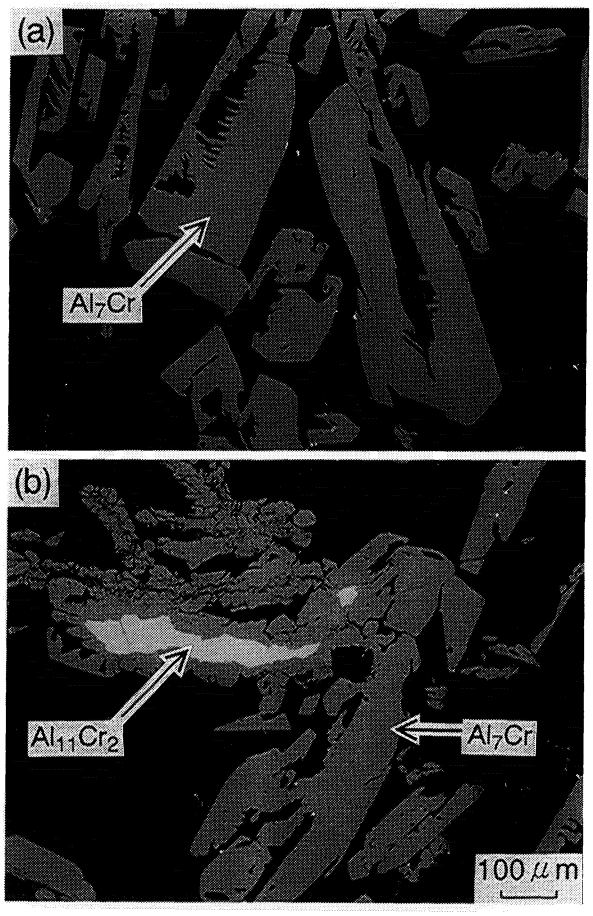

Fig. 5 Microstructures of the composite layer of the cast pipes produced by the conventional centrifugal casting (Back-scattered electron images obtained by using SEM). (a) Al-2.5 mass%Cr alloy, (b) Al-5 mass%Cr alloy.

that the primary crystal of the centrifugally cast Al-5 mass%Cr alloy is the Al_7Cr phase, citing the phase diagram proposed by Neto *et al.*[8] which denies the presence of the $Al_{11}Cr_2$ phase. Our results, however, support the phase diagram proposed by Murray[6], which is quoted in Fig. 1.

2. Solidification structures of CDC pipes

(1) Effect of the time interval of casting operations

Figure 6 gives an example of the structure of the CDC pipe. Figure 6(a) shows the macrostructure near the outer periphery, and Figs. 6(b) and (c) show the microstructures of the composite layer. This specimen was made by casting the second melt of the Al-10 mass%Cr alloy immediately before the first melt began to solidify. The time interval between the two casting operations, $\Delta\tau$, was 30 s. The mass ratio of the first melt to the second melt, W_1/W_2, was 3.

As shown in Fig. 6(a), a layer with fine, white points is observed in the outermost part of the specimen and an intermetallics free region is on the inner side. At the boundary between them, comparatively coarse particles of intermetallic compound formed. That is, the composite layer is composed of two different regions in this specimen. In the outermost area, extremely fine particles of intermetallic compound (white particles) are uniformly distributed, as shown in Fig. 6(b). This area is called the "fine composite layer". And the area where coarse intermetallic crystals are distributed is called the "coarse composite layer". Figure 6(c) shows the microstructure of the fine-coarse transition region in the composite layer. The boundary between the fine and the coarse composite layers is clear. In both layers, the intermetallic compound was detected as Al_7Cr phase. As mentioned above, the fine composite layer forms along the outer periphery of the CDC pipe. It was confirmed from these results that refinement and localization of the primary intermetallic crystals can be achieved by the CDC process. However, the size of the intermetallic crystals in the coarse composite layer is similar to that of the cast pipe produced by the conventional process. Such coarse intermetallic crystals may often act as defects causing fracture of the pipes. Therefore, it is preferable to suppress their formation. We can now propose a mechanism for the formation of the coarse composite layer as follows.

First, it should be noted that the coarse particles are distributed on the inner side of the fine composite layer. This indicates that the coarse particles crystallize after the formation of the fine composite layer. In the CDC process, the second melt comes in contact with the first melt and cools rapidly. At this point, a part of the solute chromium in the second melt diffuses into the first melt.

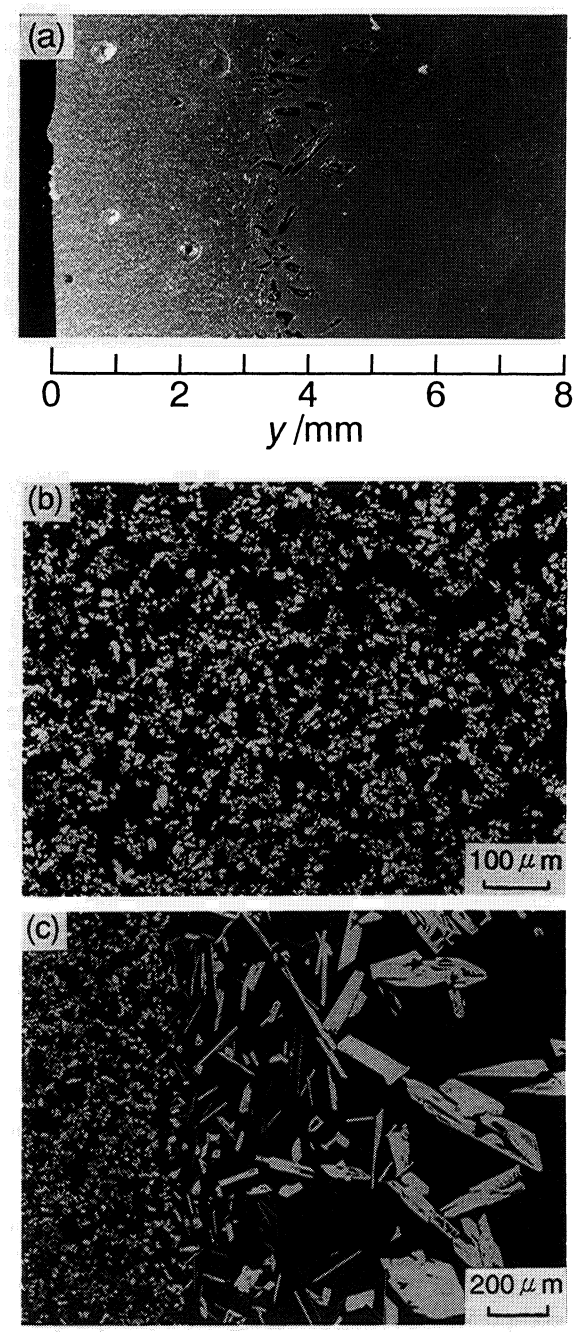

Fig. 6 Structures of the composite layer of the cast pipe produced by the CDC process. The second melt was Al-10 mass%Cr alloy. The mass ratio of the first melt to the second melt, W_1/W_2, was 3. The time interval between the two casting operations, $\Delta\tau$, was 30 s. The temperature of the first melt was just above its melting point when the second melt was cast. (a) macrostructure, (b) microstructure of the fine composite layer, (c) microstructure of the fine-coarse transition region in the composite layer.

The Cr contained in the first melt is used for the crystallization of the intermetallic compound during the cooling process of the whole specimen, after formation of the fine composite layer. Because the cooling rate at this stage is relatively slow, the intermetallic crystals can grow quite large. To minimize the diffusion of the solute chromium into the first melt, it is effective to crystallize the all of the intermetallic compound in the second melt before the diffusion process starts. To do this, it is necessary to rapidly cool the second melt below the temperature of the final peritectic reaction. Based on the above supposition, we attempted to solidify a part of the first melt before the mixing of the second melt in order to increase the cooling capacity of the first melt through the effect of latent heat absorption.

Figure 7 shows the effect of the time interval between the two casting operations, $\Delta\tau$, on the macrostructure of the CDC pipe. Figure 7(a) represents the case of $\Delta\tau=10$ s. When the second melt was cast, the first melt was still completely in the liquid state and had a superheat of 50 K. Figure 7(b) represents the case of $\Delta\tau=150$ s. This photograph was taken in a dark-field illumination. The fraction solid of the first melt at the moment of the second-melt casting, f_{S1}, was about 0.33. The value of f_{S1} was estimated with the assumption that the solidification rate, ξ, was a constant for the first melt. (We defined ξ as $W_1\, \mathrm{d}f_S/\mathrm{d}t$, where f_S is the fraction solid.) The value of ξ was estimated from the centrifugal casting experiment, in which only the first melt was cast. When we compare the three kinds of specimens from Figs. 6(a), 7(a) and (b), we can see the tendency of the coarse composite layer to shrink and the fine composite layer to expand as $\Delta\tau$ increases. Figure 8 shows a microstructure near the boundary between the composite layer and the intermetallics free region in the specimen shown in Fig. 7(b). In this specimen, the formation of the coarse composite layer

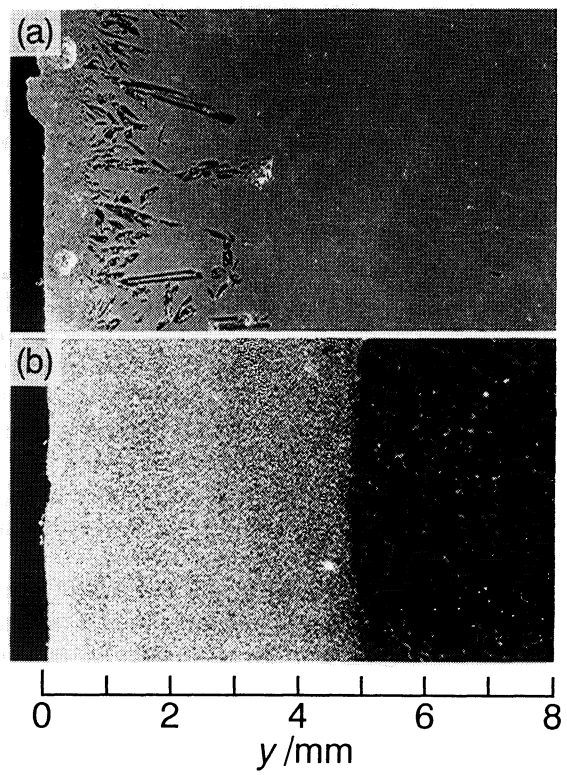

Fig. 7 Effects of the time interval, $\Delta\tau$, on the structure of the composite layer. The second melt was Al-10 mass%Cr alloy. $W_1/W_2=3$. (a) $\Delta\tau=10$ s, (b) $\Delta\tau=150$ s (photographed in a dark-field illumination).

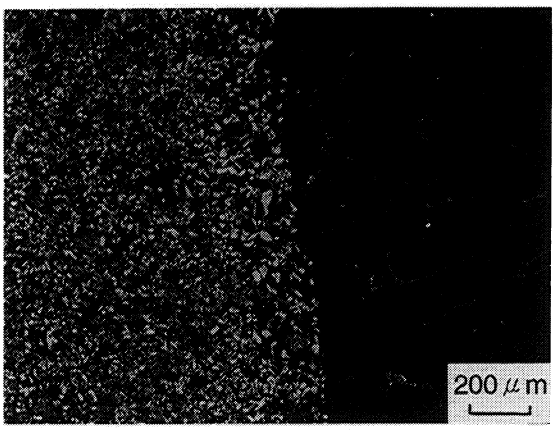

Fig. 8 Microstructure near the boundary between the composite layer and the intermetallics free region. The second melt was Al-10 mass%Cr alloy. $W_1/W_2=3$. $\Delta\tau=150$ s.

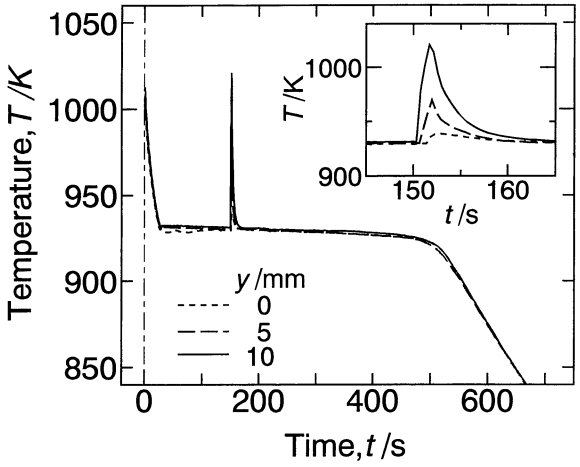

Fig. 9 Time-temperature curves measured during the CDC process. The second melt was Al-10 mass%Cr alloy. $W_1/W_2=3$. $\Delta\tau=150$ s.

was almost completely suppressed.

Figure 9 shows the time-temperature curves measured at 0, 5, 10 mm from the outer periphery of specimen shown in Fig. 7(b). The differences in temperatures at these three points are hardly seen except immediately after the mixing of the second melt. It is important to notice here that the temperature rise at the outer periphery ($y=0$ mm) due to the second melt is extremely small. This temperature rise is 10 K, which is only 4% of the solidification temperature range of the second melt. This suggests that the fluid clumps of the second melt, which passed through the first melt and reached the outer periphery, were cooled rapidly to near the final peritectic temperature. Figure 10 shows the effect of $\Delta\tau$ on the temperature change at the outer periphery after the mixing of the second melt. From these results, it can be confirmed that the temperature rise is controlled by f_{S1}, which increases as $\Delta\tau$ increases.

As mentioned above, the latent heat absorption effect increases the cooling capacity of the first melt and prevent the formation of coarse intermetallic crystals.

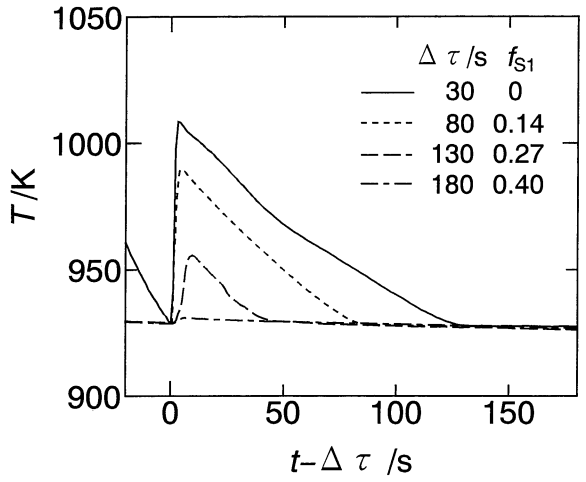

Fig. 10 Effects of the time interval, $\Delta\tau$, on the temperature change at the outer periphery ($y=0$ mm) after the second-melt casting. f_{S1}: fraction solid of the first melt at the moment of the second-melt casting.

(2) Effect of the mass ratio of the first to the second melt

Figure 11 shows a macrostructure when the mass ratio of the first melt to the second melt, W_1/W_2, is 7. The Al-10 mass%Cr alloy was used for the second melt, and f_{S1} was 0.13. The value of f_{S1} was estimated from another experiment for the centrifugal casting of the first melt, corresponding to the melt mass ratio, $W_1/W_2=7$. In Fig. 11, almost the entire area of the composite layer is a fine composite layer. The mass fraction of the first melt under these conditions is higher than in the case shown in Fig. 7(b), in which W_1/W_2 was 3. Therefore, the formation of coarse intermetallic crystals can be suppressed in spite of a smaller fraction solid. In this example, the thickness of the composite layer is about 2 mm, which is 3 mm thinner than that of the specimen shown in Fig. 7(b).

(3) Particle size and volume fraction of intermetallic crystals in the composite layer

Figures 12(a) and (b) show the distributions of the par-

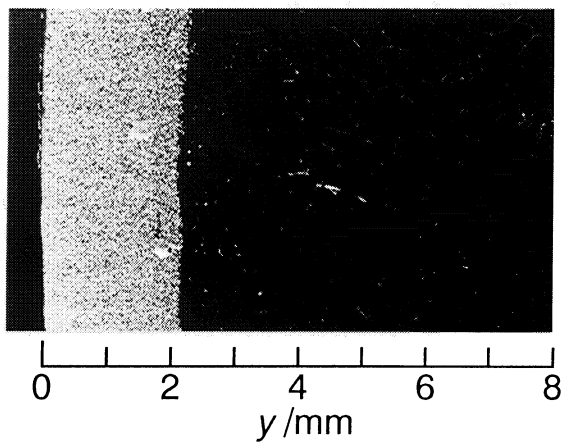

Fig. 11 Macrostructure near the outer periphery (photographed in a dark-field illumination). The second melt was Al-10 mass%Cr alloy. $W_1/W_2=7$. $\Delta\tau=85$ s.

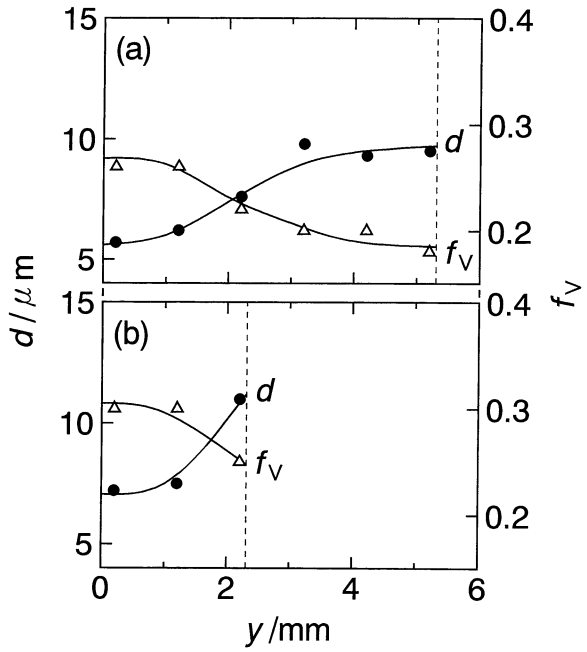

Fig. 12 Distributions of the particle size, d, and the volume fraction, f_V, of the intermetallic crystals. (a) $W_1/W_2=3$ (shown in Fig. 7(b)), (b) $W_1/W_2=7$ (shown in Fig. 11).

ticle size and volume fraction of the intermetallic crystals for the specimens shown in Figs. 7(b) and 11, respectively. The value of the particle size is the arithmetic mean of the area equivalent diameter. The broken line in each figure indicates the boundary between the composite layer and the intermetallics free region. In Fig. 12(a), the particle size gradually increases from 5 to 10 μm, and the volume fraction decreases gradually from about 0.3 to about 0.2 as the distance from the outer periphery increases. A similar tendency of graded distributions is seen in Fig. 12(b). These results show that we can control the thickness of the composite layer without significant changes in the size and volume fraction of the intermetallic crystals by adjusting the mass ratio of the first to the second melt.

(4) Effect of second-melt composition

Figure 13 shows a microstructure of the fine composite layer in the specimen produced by the CDC process with a second melt of Al-20 mass%Cr alloy. The second melt was cast just before the first melt began to solidify. The mass ratio of the first to the second melt, W_1/W_2, was 7. Clusters of fine intermetallic crystals are observed in Fig. 13. The intermetallic compound is Al_7Cr phase. Similar cluster structures are also observed on a hypereutectic Al-Si alloy ingot produced by the Duplex Casting process[7][9]. The cluster structures were formed from the fluid clumps of the second melt. In this experiment, the apparent viscosity of the fluid clumps rapidly increased during mixing because the composition of the second melt was near that of the Al_7Cr phase. As a result, the deformation of the fluid clumps and the dispersion of the intermetallic crystals became difficult. These results suggest

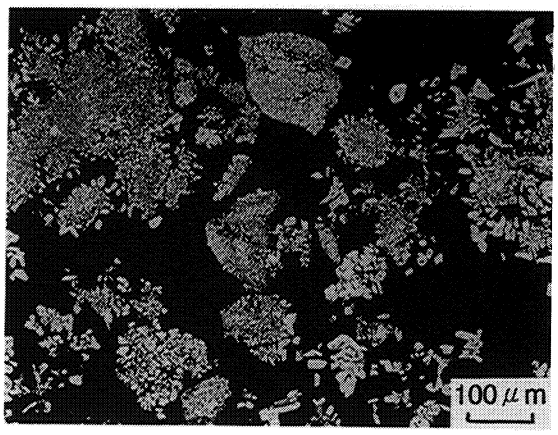

Fig. 13 Microstructure of the fine composite layer when the second melt is Al-20 mass%Cr alloy, and $W_1/W_2=7$. The temperature of the first melt was just above its melting point when the second melt was cast.

that the concept of the CDC process illustrated in Fig. 2 is appropriate.

If maintaining a uniform structure in the composite layer is a priority, the structure shown in Fig. 13 is undesirable. However, to control the volume fraction of reinforcements in composite layer, we must develop a technique for accumulating such Cr-rich clusters more densely. This is a problem which should be examined in the future.

V. Conclusions

A new process named "Centrifugal Duplex Casting" was applied to a hyperperitectic Al-Cr alloy. We attempted to fabricate a tubular surface composite which has fine intermetallic crystals on the outer periphery. The effects of the time interval between the two casting operations, the melt mass ratio, and the composition of the second melt on the structure of the surface composite layer were investigated. The results of our investigation are summarized as follows:

(1) A cast pipe with a fine composite layer along the outer periphery can be produced by Centrifugal Duplex Casting.

(2) When the cooling capacity of the first melt is insufficient, a coarse composite layer forms on the inner side of the fine composite layer. Solidifying a portion of the first melt improves its cooling capacity and can help to suppress the formation of the coarse composite layer. Therefore, the selection of an appropriate casting time interval depending on casting conditions is important for the structural control of the composite layer.

(3) By adjusting the mass ratio of the first to the second melt, the thickness of the composite layer is controlled without significant changes in the size and volume fraction of the intermetallic crystals.

(4) When the Al-10 mass%Cr alloy is used for the second melt, the dispersion of the intermetallic compound in the fine composite layer is uniform. On the

other hand, when the Al–20 mass%Cr alloy is used for the second melt, cluster structures are observed, and the distribution of the intermetallic crystals in the fine composite layer is microscopically non-uniform.

Acknowledgment

This work was supported in part by a Grant-in-Aid for Scientific Research from the Ministry of Education, Science, Sports and Culture, Japan.

REFERENCES

(1) K. Murata, M. Takada, T. Nakata and T. Umeda: IMONO, **64** (1992), 537.
(2) K. Murata, H. Harada, T. Nakata and T. Umeda: IMONO, **66** (1994), 110.
(3) Y. Fukui, N. Yamanaka, Y. Watanabe and Y. Oya-Seimiya: J. Japan Inst. Light Metals, **44** (1994), 622.
(4) J. Sugishita: IMONO, **58** (1986), 707.
(5) T. Ohmi and M. Kudoh: J. Japan Inst. Metals, **54** (1990), 700.
(6) J. L. Murray: *Binary Alloy Phase Diagrams, 2nd edition*, Ed. by T. B. Massalski, ASM, (1990), p. 138.
(7) T. Ohmi, M. Kudoh and K. Ohsasa: J. Japan Inst. Metals, **56** (1992), 1064.
(8) J. G. C. Neto, S. Gama and C. A. Ribeiro: J. Alloys and Compounds, **182** (1992), 271.
(9) T. Ohmi, M. Kudoh, K. Ohsasa, Y. Itoh and K. Matsuura: J. Japan Inst. Light Metals, **44** (1994), 91.